Ultrasonic microspectroscopy characterization of silica glass

doi: 10.1063/1.372307

Ultrasonic microspectroscopy characterization of silica glass

Jun-ichi Kushibiki, Ting-Cun Wei, Yuji Ohashi, and Akira Tada
Department of Electrical Engineering, Tohoku University, Sendai 980-8579, Japan

(Received 16 August 1999; accepted for publication 7 December 1999)

Ultrasonic microspectroscopy technology, using the line-focus-beam and plane-wave ultrasonic material characterization system, is applied to characterization of silica glass. Eight types of commercial silica glasses fabricated by different production methods and conditions are used as specimens to measure their acoustic properties accurately, *viz.*, acoustic velocity, density, elastic constant. The variations in those acoustic properties resulting from small amounts of impurities, such as hydroxyl (OH) and chlorine, incorporated during the production processes were quantitatively obtained. The longitudinal velocity, density, and elastic constant c_{11} of silica glass with 860 ppm OH ions were less by 0.28%, 0.06%, and 0.62%, respectively, than those for OH-free silica glass, while the temperature coefficient of the longitudinal velocity was greater by 7.4%. In contrast, the leaky surface acoustic wave velocity, shear velocity and elastic constant c_{44} of silica glass containing 1500 ppm residual chlorine were less by 0.23%, 0.30%, and 0.59%, respectively, than those of OH-free and chlorine-free silica glass, while the longitudinal velocity, elastic constant c_{11}, and density increased slightly by 0.04%, 0.10%, and 0.02%, respectively. Further, it was found that the decrease in acoustic velocity due to OH or chlorine is mainly related to the decrease in the elastic constant, which also corresponds to the decrease in the viscosity of the SiO_2 material. These results demonstrate that the ultrasonic method is very useful and effective for analyzing and evaluating both the glass properties and the production processes. © *2000 American Institute of Physics.* [S0021-8979(00)05606-1]

I. INTRODUCTION

Pure silica glass has excellent optical transmission properties and is widely used as optical waveguide material in optical fibers and planar lightwave circuits for telecommunications.[1–4] Moreover, as this material has excellent heat and thermal shock resistance and chemical durability, it is used in a wide variety of applications in science and industry.[5]

Silica glass is broadly divided into fused quartz glass and synthetic silica glass, depending upon the fabrication method.[5] Fused quartz glass is produced from natural quartz powder into amorphous glass by electrical fusion or oxygen-hydrogen flame fusion. In contrast, synthetic silica glass is produced through the hydrolysis of ultrahigh-purity silicon tetrachloride ($SiCl_4$) in an oxygen-hydrogen flame. There are two types of synthetic silica glasses: one is made by the direct method in which silica is directly deposited and consolidated at a high temperature; the other is made by the soot method, e.g., the vapor phase axial deposition (VAD) method,[6] in which porous silica preform is prepared at a relatively low temperature and then consolidated at a high temperature.

A small amount of impurity, such as metallic elements (Al, Ca, Na, Ti, etc.), hydroxyl (OH), and chlorine (Cl) ions, are incorporated into silica glass in the fabrication processes, and affect its properties depending upon the concentrations.[5] For example, OH ions generate an optical absorption band in the infrared region, which determines the minimum intrinsic loss in silica optical fiber.[3] Further, the OH ion content is one of the most important parameters for evaluating the quality and characteristics of silica glass because OH ions are related to various physical and optical properties of silica glass, such as viscosity at high temperatures,[7,8] Rayleigh scattering loss,[9] and excimer laser resistivity.[10,11] Its properties are also considered to vary greatly with thermal history. Thus, development of proper methods and systems for precisely characterizing the silica glass and evaluating the fabrication processes are needed in order to assure acceptable products.

The acoustic properties of glasses depend strongly upon the chemical composition and fabrication processes, and are closely related to other physical and chemical properties.[5,12–21] The acoustic information is, therefore, very useful for property analysis and evaluation of glass materials. Ultrasonic microspectroscopy (UMS) technology, primarily employing the line-focus-beam (LFB) acoustic microscopy system[22] with a function of bulk-wave measurements, enables us to measure accurately the propagation characteristics of leaky surface acoustic waves (LSAW) propagating on the water-sample boundary, and the bulk acoustic properties. This UMS technology has the capability of nondestructive and noncontacting evaluation of material properties at the microscopic level and has been applied to property analysis and evaluation of various glasses.[23–27]

In this article, ultrasonic characterization of silica glasses by the UMS technology is reported. Eight types of commercial silica glasses produced by different fabrication methods and/or conditions are taken as specimens. Changes in the acoustic properties due to small amounts of impurities such as OH ions and chlorine, are examined thoroughly to dem-

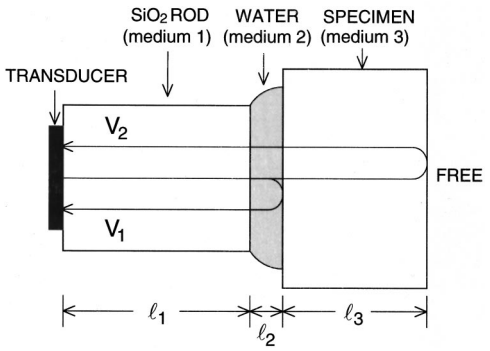

FIG. 1. Experimental arrangement for longitudinal velocity measurements by the double-pulse interference method.

onstrate the usefulness and effectiveness of the characterization and evaluation of glass materials and their fabrication processes using this ultrasonic method.

II. MEASUREMENT METHODS

The LFB and plane-wave (PW) ultrasonic material characterization (UMC) system recently developed[28] is used to measure the acoustic velocity of the silica glass specimens, which have the acoustic properties of very small propagation attenuation and no velocity dispersion in the ultrasonic frequency range used in this study. The methods of measuring the velocities of LSAW, longitudinal, and shear waves are described below. As the density is needed to determine the stiffness constants from the measured velocity data, it is measured with an accuracy better than ± 0.1 kg/m^3 based on the Archimedes method,[29] using the density of pure water as the reference.

A. Longitudinal velocity

The measurement method for the longitudinal velocity was described in detail in the literature.[30,31] Figure 1 shows the configuration as an ultrasonic transmission line system for measuring longitudinal velocities. Pure water, as a coupling medium, is poured into the gap space between the solid specimen and the ultrasonic device consisting of a ZnO piezoelectric thin-film transducer formed on one end face of a buffer rod of synthetic silica glass. The measurement is performed using rf tone burst pulse signals. In Fig. 1, the transducer output voltages V_1 and V_2, in response to the reflection signals from the top and back surfaces of the specimen, are expressed by the following:

$$V_1 = AT_{12}R_{23}T_{21}ATT_1 \exp(-2\gamma_1 l_1 - 2\gamma_2 l_2), \tag{1}$$

$$V_2 = AT_{12}T_{23}R_{\text{free}}T_{32}T_{21}ATT_2 \times \exp(-2\gamma_1 l_1 - 2\gamma_2 l_2 - 2\gamma_3 l_3). \tag{2}$$

Here, A is an arbitrary amplitude, R_{ij} and T_{ij} are the reflection and transmission coefficients for the ultrasonic waves propagating from medium i to medium j, R_{free} is -1, l_i is the length of medium i, γ_i $(=\alpha_i + j\beta_i$, where α_i is the attenuation coefficient, and β_i is the phase constant) is the propagation constant of medium i, and ATT_i $(=|ATT_i|\exp(j\theta_i)$, where $|ATT_i|$ is the diffraction loss, and θ_i is the phase advance) represents the diffraction effect[32] along the propagation path for the transducer output V_i, where $i=1,2$.

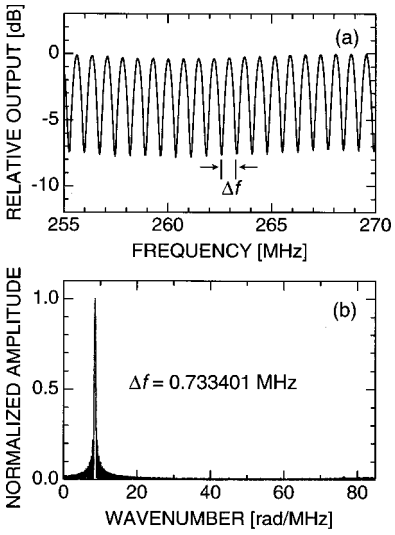

FIG. 2. Longitudinal velocity measurement for synthetic silica glass (sample ES). (a) Interference wave form obtained by the double-pulse interference method; (b) final spectral distribution analyzed by FFT for the wave form shown in (a).

The longitudinal velocity is measured by the double-pulse interference method. In Fig. 1, the reflected signals V_1 and V_2 overlap in the time domain so that they interfere with each other. When the ultrasonic frequency is swept, its interference output repeats the local maximum and minimum values periodically, according to the change in the phase difference between V_1 and V_2, in which an interference wave form, as shown in Fig. 2(a), is obtained. When diffraction is ignored, the velocity V_l of the specimen is determined using

$$V_l = 2l_3\Delta f, \tag{3}$$

where Δf is the frequency interval in the interference wave form and l_3 is the specimen thickness. The value of Δf, as shown in Fig. 2(b), is obtained by performing a fast Fourier transform (FFT) analysis of the interference wave form, shown in Fig. 2(a), and l_3 is measured using a digital length gauging system with an accuracy of ± 0.1 μm. The accuracy in velocity measurements is with the maximum measurement error of ± 0.3 m/s, which is mainly determined by the thickness measurement accuracy and the diffraction effect.[32,33]

B. LSAW velocity

The measurement principle of the LSAW velocity has been described in detail elsewhere.[22] The LFB–UMC system is used to obtain the propagation characteristics, *viz.*, velocity and attenuation, of LSAWs, excited on the water-loaded specimen surface through the measurement and analysis of the $V(z)$ curves and to evaluate the acoustic properties near the specimen surface. We use the velocity data. Figure 3 is a schematic cross section of the LFB ultrasonic device and specimen system, which illustrates the formation of the $V(z)$ curve. Ultrasonic plane waves excited by the transducer are focused by the cylindrical lens surface, formed into a wedge-

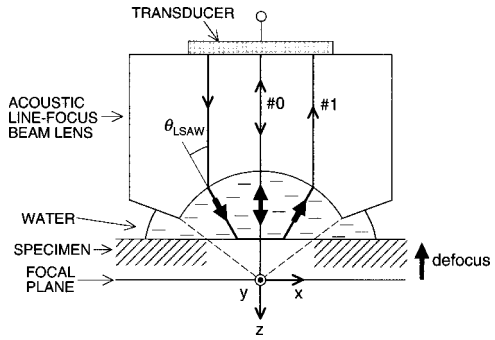

FIG. 3. Cross-sectional geometry of acoustic LFB lens and specimen, explaining the construction mechanism of $V(z)$ curve obtained by LFB acoustic microscopy.

shaped ultrasonic beam, and focused on the specimen surface through the water as a couplant. When the distance z between the acoustic lens and the specimen is varied, the two components, #0 and #1, interfere with each other to form an interference wave form called the $V(z)$ curve. Figure 4(a) shows the typical $V(z)$ curve measured for a synthetic silica glass (sample ES) at an ultrasonic frequency of 225 MHz. The oscillation interval Δz is determined according to the $V(z)$ curve analysis procedure in Fig. 4(b). The LSAW velocity V_{LSAW} is obtained from the following equation:

$$V_{\mathrm{LSAW}}=\frac{V_w}{\sqrt{1-\left(1-\dfrac{V_w}{2f\Delta z}\right)^2}}, \tag{4}$$

where f is the ultrasonic frequency and V_w is the longitudinal velocity in water.

Measured LSAW velocity values depend on the performance characteristics of the ultrasonic device and the measurement system used. To eliminate this influence, the measured value of the LSAW velocity must be calibrated absolutely using the standard specimen of synthetic silica glass (T-4040, Toshiba Ceramics Co., Ltd.).[30] It is estimated that the absolute measurement accuracy of LSAW velocities is around $\pm 0.01\%$, and the relative accuracy is better than $\pm 0.005\%$ for a single measurement.[30]

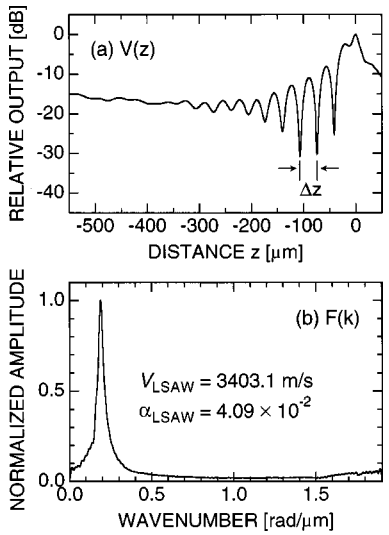

FIG. 4. $V(z)$ curve analysis for synthetic silica glass (sample ES). (a) Typical $V(z)$ curve measured at 225 MHz; (b) final spectral distribution analyzed by FFT for the $V(z)$ curve shown in (a).

C. Shear velocity

The shear velocity is determined through numerical calculations from measurements of the LSAW velocity, longitudinal velocity, and density using the technique described in the Ref. 24. This technique enables determination of the shear velocity indirectly, but without bonding specimens to any device.

The LSAW propagation characteristics is given as the complex wave number k, which satisfies the following characteristic equation:[34,35]

$$4\beta_1\beta_2-(1+\beta_2^2)^2=-\frac{\rho_w}{\rho}\frac{\beta_1}{\beta_3}(1-\beta_2^2)^2, \tag{5}$$

where,

$$\beta_1=\sqrt{1-\left(\frac{k_l}{k}\right)^2}, \quad \beta_2=\sqrt{1-\left(\frac{k_s}{k}\right)^2},$$

$$\beta_3=\sqrt{1-\left(\frac{k_w}{k}\right)^2}, \quad k=\frac{\omega}{V_{\mathrm{LSAW}}}(1+j\alpha_{\mathrm{LSAW}}),$$

ρ and ρ_w are the densities of the specimen and water, k_l and k_s are the wave numbers of the longitudinal and shear waves in the specimen, and k_w is the wave number of the longitudinal wave in water.

III. SPECIMENS

Eight types of commercial silica glasses manufactured by different fabrication methods and conditions (Nippon Silica Glass Co., Ltd.) were used for measurements: three fused quartz glasses made from natural quartz powder by oxygen-hydrogen flame fusion (type II silica glass, N and NP) and by electrical fusion (type I silica glass, HRP), and five synthetic silica glasses made by hydrolyzation of $SiCl_4$ (type III silica glass, ES) and by the VAD method without any complete dehydration (ED–A and ED–H) and with dehydration (ED–B and ED–C). The types and concentrations of impurities in each specimen are listed in Table I. The OH content was determined by infrared spectrophotometery. The concentration of chlorine was measured using the x-ray fluorescence analysis method. The data of the concentrations of metallic impurities are the values published by the manufacturer.[8,11]

Table I shows that fused quartz glasses have higher concentrations of metallic impurities than do synthetic silica glasses. Since fused quartz glasses are produced by fusing natural quartz powder, metallic impurities are incorporated into them from the raw source material and also from the crucible used in the fabrication process. In contrast, for syn-

TABLE I. Impurity of silica glass specimens. (Unit: ppm).

Type	Sample	Al	Ca	Cu	Fe	Na	K	Li	Mg	Mn	Ti	OH	Cl
Fused	N	9	0.6	0.03	0.4	0.6	0.3	0.2	0.2	<0.01	1.6	187	···
Quartz	NP	8	0.5	0.01	0.1	0.1	0.1	0.1	0.2	<0.01	1.5	170	···
Glass	HRP	9	0.6	0.01	0.3	0.1	0.3	0.1	0.2	<0.01	1.1	8	···
	ES	0.1	0.1	0.01	0.05	0.05	0.05	0.05	<0.01	<0.01	<0.01	860	30
Synthetic	ED–A	<0.01	<0.01	<0.01	<0.01	<0.01	<0.01	<0.01	<0.01	<0.01	<0.01	64	···
Silica	ED–H	<0.01	<0.01	<0.01	<0.01	<0.01	<0.01	<0.01	<0.01	<0.01	<0.01	48	···
Glass	ED–B	<0.01	<0.01	<0.01	<0.01	<0.01	<0.01	<0.01	<0.01	<0.01	<0.01	<1	···
	ED–C	<0.01	<0.01	<0.01	<0.01	<0.01	<0.01	<0.01	<0.01	<0.01	<0.01	<1	1500

thetic silica glasses, since they are synthesized in the vapor phase, the ultrahigh purity of the starting materials are made use of.

The OH content is highest in the ES synthetic silica glass made by hydrolyzation of $SiCl_4$, and followed by the N and NP fused quartz glasses made by oxygen-hydrogen flame fusion, because H_2O is formed by the oxygen-hydrogen burner used for producing these two types of glasses.[5] The synthetic silica glasses made by the VAD method have a relatively low OH content, particularly ED–B and ED–C synthetic silica glasses made by the VAD method with an almost complete dehydration process, having less than 1 ppm OH content. Residual chlorine exists in ES and ED–C glasses, which is thought to be incorporated for ES glass from the starting material ($SiCl_4$) and for ED–C glass from the processing gas (Cl_2) used for dehydration.[36] For ED–A synthetic silica glasses, no dehydration process is involved, and, for ED–H and ED–B synthetic silica glass, some different processing gases are used for dehydration, but no residual atomic elements were detected by x-ray fluorescence analysis and electron probe microanalysis.

From Table I, it is clear that the effects of the OH, chlorine, and metallic impurities on the acoustic properties must be examined.

Each specimen studied had dimensions of $50\,\text{mm}\times50\,\text{mm}\times4\,\text{mm}$ with both major faces optically polished and parallelism to less than 10 seconds.

IV. RESULTS

Using the measurement methods and systems described earlier, the densities, longitudinal velocities, and LSAW velocities were measured, and are shown in Table II. The longitudinal velocities of each specimen were measured in the frequency range 80–300 MHz, so that no specimen exhibited any suggestion of velocity dispersion, having a constant velocity value. The longitudinal velocities were measured as a function of temperature in the range 20–26 °C, shown in Fig. 5. From these data, the temperature coefficients around 23 °C were determined using a linear approximation by the least squares method for the three measured values of each specimen, which also illustrates the precision of the measurements. The results are presented in Table II. The stiffness elastic constants c_{11} and c_{44} are calculated from the measured values of longitudinal velocity V_l, shear velocity V_s, and density ρ at 23.0 °C, using the equations $c_{11}=\rho V_l^2$ and $c_{44}=\rho V_s^2$, respectively, (Table II).

We are, in this article, trying to find some relationships among the acoustic properties, *viz.*, velocity, temperature coefficient, density, elastic constants, and the impurities, i.e., OH, chlorine, and metallic ions, actually detected. It is clear from Fig. 5 and Table I that sample ES exhibits the least longitudinal velocity and the greatest temperature coefficient among the eight specimens, which may be related to its OH content of 860 ppm. Thus, attention must be devoted to try-

TABLE II. Acoustic properties measured for silica glasses at 23.0 °C.

Type	Sample	OH content (ppm)	Density (kg/m^3)	Longitudinal velocity V_l (m/s)	dV_l/dT [m/s/°C] (20–26 °C)	Shear velocity V_s (m/s)	LSAW velocity V_{LSAW} (m/s)	Stiffness elastic constant ($\times10^{10}\,\text{N/m}^2$) c_{11}	c_{44}
Fused	N	187	2202.0	5959.2	0.696	3767.5	3429.7	7.8197	3.1255
Quartz	NP	170	2201.8	5958.5	0.660	3767.6	3429.7	7.8171	3.1254
Glass	HRP	8	2202.5	5962.5	0.685	3767.1	3429.8	7.8303	3.1256
	ES	860	2200.6	5940.6	0.740	3764.4	3425.3	7.7660	3.1183
Synthetic	ED–A	64	2202.6	5963.3	0.678	3765.8	3429.0	7.8326	3.1236
Silica	ED–H	48	2202.5	5961.3	0.667	3766.8	3429.4	7.8269	3.1250
Glass	ED–B	<1	2202.0	5957.0	0.688	3768.9	3430.4	7.8140	3.1279
	ED–C	<1	2202.5	5959.3	0.663	3757.5	3422.5	7.8215	3.1095

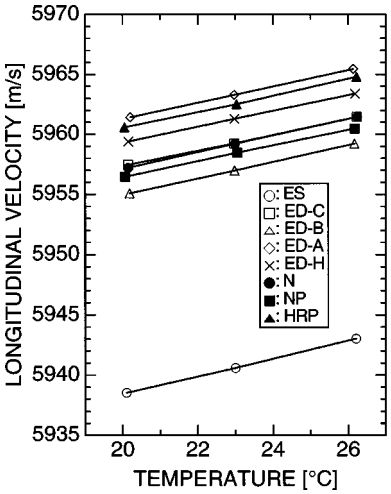

FIG. 5. Measured longitudinal velocities as a function of temperature in the range of 20–26 °C.

ing to understand the effect of the OH ions, as a common and important factor for influencing the acoustic properties. Therefore, the data were first plotted as a function of OH ion content and shown in Figs. 6–11. Although the OH contents of ED–B and ED–C were less than the limit of detection of 1 ppm, they are plotted as 1 ppm on the figures. In each figure, the data for the specimens were plotted as a function of OH ion content by dividing them into three groups, *viz.*, for the fused quartz glasses (N, NP, and HRP) marked as closed circles, for the synthetic silica glasses (ED–A, ED–B, and ED–H) containing some OH ions marked as open circles, and for the synthetic silica glasses (ES and ED–C) containing the additional impurity of chlorine marked as double circles.

The following emerges from examination of the acoustic results with the data of chemical impurities in Table I. The acoustic properties of sample ED–C containing 1500 ppm chlorine differ considerably from those of sample ED–B, so effect of chlorine on the acoustic properties of SiO_2 will be discussed first in the next section. The acoustic properties of sample ES is considered to be influenced by its high OH ion content, and will be examined second. It is seen that the acoustic properties of samples N and NP, and of samples ED–A and ED–H are roughly the same, possibly because of the nearly same chemical compositions and production methods, although differences in the acoustic properties are significantly detected from the technical viewpoint of measurement accuracy. The effects of the metallic impurities will be discussed last.

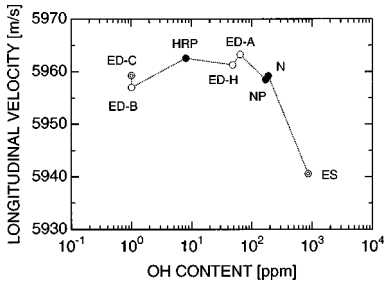

FIG. 7. OH content dependences of longitudinal velocities at 23.0 °C.

V. DISCUSSIONS

A. Chlorine effect

First, we take notice of the acoustic properties of samples ED–B and ED–C to discuss the effect of chlorine incorporated during the dehydration process. Large differences are observed in the acoustic properties, as shown in Figs. 6–11, although the OH contents are nearly the same between them: less than 1 ppm. The changes in the acoustic properties may result from the difference in atmospheric gas used in the dehydration process. It is obvious that the dehydration process in VAD fabrication of ED–C and ED–B type glasses was performed. We detected chlorine of 1500 ppm for sample ED–C by x-ray fluorescence analysis, although nothing for sample ED–B was observed by x-ray fluorescence analysis and electron probe microanalysis. We now make an assumption that all the changes in the acoustic properties between samples ED–B and ED–C are due to the residual chlorine of 1500 ppm.

From Table II, we can calculate that the chlorine increases the density by 0.5 kg/m^3 (0.02%), the longitudinal velocity by 2.3 m/s (0.04%), and c_{11} by 0.75×10^8 N/m^2(0.10%), while it decreases dV_l/dT, by 0.03 (m/s)/°C (4.35%) at 23 °C, the shear velocity by 11.4 m/s (0.30%), the LSAW velocity by 7.9 m/s (0.23%), and c_{44} by 1.84×10^8 N/m^2(0.59%). So, the sensitivities of each acoustic parameter of SiO_2 glass to chlorine are estimated to be +3.33 (kg/m^3)/wt % in density, +15.3 (m/s)/wt % in longitudinal velocity, −0.20 (m/s),/°C/wt % in dV_l/dT, −76.0

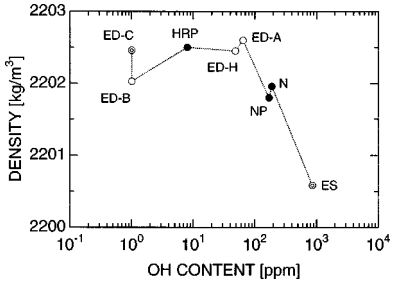

FIG. 6. OH content dependence of density at 23.0 °C.

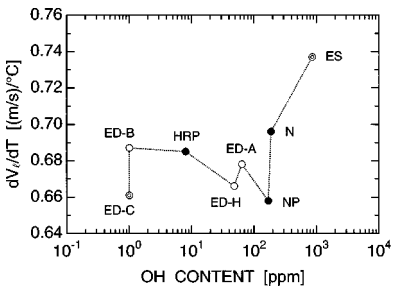

FIG. 8. OH content dependence of temperature coefficient of longitudinal velocity around 23 °C.

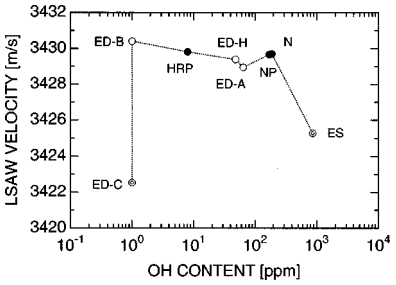

FIG. 9. OH content dependence of LSAW velocity at 23.0 °C.

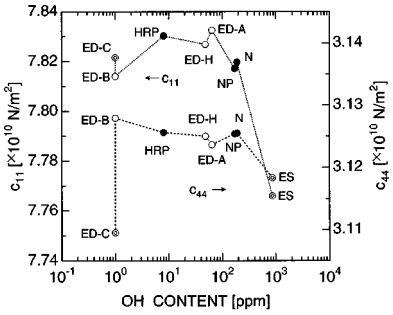

FIG. 11. OH content dependences of stiffness elastic constants at 23.0 °C.

(m/s)/wt % in shear velocity, −52.7 (m/s)/wt % in LSAW velocity, $+5.0\times10^8$ (N/m^2)/wt % in c_{11}, and -12.3×10^8 (N/m^2)/wt % in c_{44}.

It can be easily understood that the acoustic properties are greatly influenced by the residual chlorine in sample ED–C, typically indicating that the density of sample ED–C is 0.5 kg/m^3 greater than that of sample ED–B. It can also be understood, from the results shown earlier, that the chlorine contained in synthetic silica glasses influences the acoustic properties of LSAW and shear wave velocities, elastic constant c_{44}, and dV_l/dT. The residual chlorine decreases the LSAW velocity of silica glass at a rate of −52.7 (m/s)/wt %, which is in good agreement with the data of −47 (m/s)/wt % obtained previously for an optical fiber preform.[37]

Using the results obtained earlier, we can estimate the effects of chlorine of 30 ppm contained in sample ES on the acoustic properties. Therefore, the slight corrections for the LSAW velocity of 0.16 m/s and for the shear velocity of 0.23 m/s must be made.

B. OH ion effect

We try to estimate the effects of OH ions on the acoustic properties of synthetic silica glasses using the linear approximation for the data of the acoustic properties of sample ED–B and those of sample ES corrected for the residual chlorine. The effect of the OH content of 860 ppm decreases the density by 1.4 kg/m^3 (0.06%), the longitudinal velocity by 16.4 m/s (0.28%), the shear velocity by 4.3 m/s (0.11%), the LSAW velocity by 4.9 m/s (0.14%), c_{11} by 4.82×10^8 N/m^2 (0.62%), and c_{44} by 0.92×10^8 N/m^2 (0.30%), while it increases dV_l/dT by 0.051 (m/s)/ °C (7.4%) at 23 °C. Then, the following sensitivities of each acoustic parameter of SiO_2 glass to OH ion content were estimated as −16.4 (kg/m^3)/wt % in density, −191.2 (m/s)/wt % in longitudinal velocity, +0.590 (m/s/ °C)/wt % in dV_l/dT, −49.7 (m/s)/wt % in shear velocity, −57.5 (m/s)/wt % in LSAW velocity, -56.0×10^8 (N/m^2)/wt % in c_{11}, and -10.7×10^8 (N/m^2)/wt % in c_{44}. From these results, it was found that the OH ions decrease the value of most of the acoustic properties, except for the temperature coefficient, greatly influencing the changes of the longitudinal properties, including the temperature coefficient, rather than those of the shear properties. It is very interesting that the temperature coefficient of the longitudinal velocity varies greatly with the OH content.

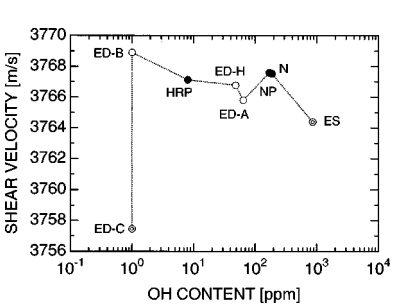

FIG. 10. OH content dependence of shear velocity at 23.0 °C.

C. Other impurity effects

Next, we examine the influence of metallic impurities other than chlorine and OH ions on the acoustic properties. As shown in Table I, the concentration of metallic impurities contained in each specimen is considerably less than that of chlorine or OH ions. Further, synthetic silica glasses have considerably lesser concentrations of metallic impurities than fused quartz glasses. Even for fused quartz glasses, the concentration of Al, which is the largest component detected as impurities, is less than 10 ppm. Nassau *et al.* have investigated the Al_2O_3 concentration dependence of the longitudinal and shear velocities of silica glasses.[21] Using their data, it is estimated that the increments of longitudinal and shear velocities caused by the content of 10 ppm Al are 0.071 and 0.021 m/s, respectively. Jen *et al.* have investigated the Al_2O_3 concentration dependence of LSAW and leaky surface skimming compressional wave (LSSCW) velocities for silica glasses.[26] Using their data, it is estimated that the increments of LSSCW and LSAW velocities caused by the 10 ppm Al content are 0.095 and 0.027 m/s, respectively. These values are nearly equal to the increments of the bulk acoustic velocities noted earlier, possibly because the main displacement components of LSSCW and LSAW are the longitudinal wave and shear wave components, respectively.[26] According to the earlier discussions, even for fused quartz glasses having about 10 ppm Al, the variations of acoustic velocities are less than 0.1 m/s, which is within the measurement errors of the acoustic velocities. The influence of other metallic impurities can be ignored because their concentrations are less than 1/10 that of Al.

TABLE III. Typical data of viscosity at 1200 °C, and strain and annealing points of silica glass specimens.

Type	Sample	Cl content (ppm)	OH content (ppm)	Viscosity at 1200 °C log (η/poise)	Strain point (°C)	Annealing point (°C)
Fused	N	···	187	13.0	1070	1180
Quartz	NP	···	170	13.0	1070	1180
Glass	HRP	···	8	13.4	1120	1220
	ES	30	860	11.7	970	1080
Synthetic	ED–A	···	64	12.8	1050	1150
Silica	ED–H	···	48	13.0	1060	1170
Glass	ED–B	···	<1	13.2	1110	1200
	ED–C	1500	<1	12.9	1070	1180

D. Changes in elastic properties

Here, we consider the variations of acoustic velocity, elastic constant, and density caused by the OH ions. From the equation $V=(c/\rho)^{1/2}$, the relationship among the variations of acoustic velocity, elastic constant, and density are given by

$$\frac{dV}{V}=\frac{1}{2}\left(\frac{dc}{c}-\frac{d\rho}{\rho}\right). \tag{6}$$

This equation states that V decreases when c decreases, but V increases when ρ decreases. The longitudinal velocity, elastic constant c_{11}, and density of sample ES were less than those of sample ED–B by 0.28%, 0.62%, and 0.06%, respectively, as described in this Sec. V B. The variation of elastic constant c_{11} was ten times as large as that of the density. This fact indicates that the decrease of the longitudinal velocity due to the OH ion content is mainly attributable to the decrease in the values of the elastic constant c_{11}. Similarly, the shear velocity, elastic constant c_{44}, and density of sample ES were less than those of sample ED–B by 0.11%, 0.30%, and 0.06%, respectively. The variation of the elastic constant c_{44} was five times as large as that of the density, so that the decrease of the shear velocity due to the OH ions is mainly attributable to the decrease of elastic constant c_{44}. We can, therefore, say that the decrease of the elastic constants is the dominant cause of the decrease of the acoustic velocities in both synthetic silica glasses and fused quartz glasses, associated with the incorporation of OH ions.

Similar discussions hold for the residual chlorine, which also greatly influences the acoustic parameters. The density of sample ED–C containing the impurity of 1500 ppm chlorine is 0.5 kg/m^3 (0.02%) greater than that of sample ED–B, although sample ED–C has the nearly same OH content less than 1 ppm as sample ED–B. While the elastic constant c_{11} slightly increases by 0.10%, the elastic constant c_{44} significantly decreases by 0.59%. So, the 1500 ppm chlorine inclusion had a great influence on the shear properties, in comparison with the influence of the 860 ppm OH ions inclusion, which gave rise to the changes in the longitudinal properties rather than those in the shear properties.

The longitudinal velocities increased linearly as the temperature rose, exhibiting elastic anomalies.[14–16] Further, it seems that the temperature coefficient increases significantly when the OH content exceeds about 200 ppm. The temperature coefficient of sample ES is 7.4% greater than that of sample ED–B. The difference (>4%) between the coefficients of samples ED–B and ED–C might be meaningful, due to the chlorine content.

E. Correspondence to viscosity changes

It has been reported that, when chlorine and OH ions are incorporated into pure silica glass (SiO_2), its continuous network, composed of SiO_4 tetrahedra, and covalent bondings are partially broken, resulting in the formation of nonbridging oxygen, so that the connectivity of the structure of silica glass becomes softer and its viscosity at high temperatures decreases.[5,7,8] Here, we attempt a discussion of the relationship between the obtained acoustic data and the other typical published data of viscosities at 1200 °C, and temperatures of the strain and annealing points for each SiO_2 glass specimen[8,11] (see Table III).

It is noted that sample HRP has the highest strain and annealing points, and the largest viscosity value among all samples, so that this type of fused quartz glass is most suitable for applications requiring for excellent heat and thermal shock resistance. As the OH content increases, the viscosity monotonically decreases for both types of fused quartz and synthetic silica glasses. However, the value for fused quartz glass is slightly, but significantly, larger at the same OH content than that for synthetic silica glass.[8,11] This difference was closely associated with the granular structure in fused quartz and consequently inhomogeneous OH distribution localized at the grain boundaries, although synthetic silica glass is rather homogeneous in its OH distribution because of the production method.[5,10] Samples N and NP have the same level in OH content, containing 160–180 ppm larger content than sample HRP, so that they have lesser viscosities due to the softening of the structure. So, we can relate the viscous effect of the OH content to the acoustic decreases of the longitudinal properties of V_l, c_{11}, and ρ, as described in Sec. V C.

Next, we examine the properties of synthetic silica glasses. Sample ED–B, among the synthetic silica glass specimens, has the property of excellent heat resistance because of high strain and annealing points, following sample HRP. The same OH content dependences of the acoustic parameters as those for the fused quartz glasses result in the decrease of each parameter. The effect of chlorine is also

TABLE IV. Resolutions to Cl, OH, and viscosity at 1200 °C.

Mode	Impurity (ppm)		Viscosity at 1200 °C [log (η/poise)]	
	Cl	OH	Cl	OH
Longitudinal wave	195.7	15.7	0.039	0.027
LSAW	57.0	52.2	0.011	0.091

significant for sample ED–C, showing the decreases in the viscosity and the strain and annealing points,[7] which correspond to the decreases in the shear properties. Therefore, it can be explained that the differences in viscosity and in strain and annealing points between samples ED–B and ED–C are due to the chlorine content.

We have a very good understanding of the correspondence between the acoustic changes and the structural changes for the effects of both OH and chlorine. Here, we can obtain the sensitivities to the viscosity due to the OH and chlorine contents using the acoustic data for samples ED–B, ED–C, and ES from the previous similar discussions of the acoustic parameters. We calculated the sensitivities of $+11.0$ (m/s)/(log$\updownarrow\eta$/poise) in longitudinal velocity, $+3.22\times10^8$ (N/m^2)/(log η/poise) in c_{11}, and $+0.94$ (kg/m^3)/(log η/poise) in density for the OH content, and the sensitivities of $+26.3$ (m/s)/(log η/poise) in LSAW velocity, $+6.14\times10^8$ (N/m^2)/(log η/poise) in c_{44}, and -1.67 (kg/m^3)/(log η/poise) in density for the chlorine content. Thus, we can evaluate the viscosity using the acoustic data together with the information of OH ion and chlorine concentrations obtained by chemical analyses.

F. Resolutions for Cl, OH, and viscosity

Using the data obtained earlier, we summarize here the resolutions by the measurements of longitudinal wave and LSAW velocities in the UMS technology for the chlorine and OH concentrations, and for the viscosity at 1200 °C for each of chlorine and OH, in Table IV.

VI. CONCLUSIONS

In this article, we conducted basic investigations to characterize silica glass and to evaluate its fabrication processes using UMS technology, using eight types of commercial silica glasses produced by different fabrication methods and conditions. Highly accurate measurements of their acoustic properties around room temperature 20–26 °C clearly revealed that the acoustic properties sensitively change responding to small amounts of impurities such as OH and chlorine ions incorporated during the fabrication processes.

In general, acoustic properties remain nearly constant when the OH content is 200 ppm or less, but exceeding 200 ppm OH content, the acoustic velocity, density, and elastic constant decrease while the temperature coefficient of longitudinal velocity increases. We observed that residual chlorine significantly decreases the shear velocity and elastic constant c_{44}, but slightly increases the density, longitudinal velocity, and elastic constant c_{11}. Further, it was clarified that the decrease of acoustic velocity due to OH and chlorine ions is primarily related to the decrease of the elastic constant, not to the density change, and also corresponds to the decrease of the viscosity. These changes of the acoustic properties reflect the tiny variations in composition or purity and the differences in the fabrication processes and conditions for silica glass products, and must be closely related to some changes in other physical properties of silica glass, such as refractive index, optical absorption, and viscosity. It is a new and very interesting finding that the OH content mainly influences the longitudinal properties, while the chlorine content mainly influences the shear properties, suggesting their different contributions to the structural strength.

With the data obtained in Sec. V, after removing the effects of residual chlorine and OH ion content, and neglecting the effects of other impurities, some changes, still observed in the acoustic properties, might possibly be considered to be due to other residual chemical elements, not detected in this study, some differences in thermal history during the production processes, and some structural factors such as striae and granularity in fused quartz glasses.[5] Further studies are required.

This ultrasonic method presents unique and important information for investigating scientific glass material problems and for developing optimal control and improvement of the fabrication processes and conditions for all kinds of glasses, as well as for silica glasses.

ACKNOWLEDGMENTS

The authors would like to express our gratitude to H. Sudo and E. Abe of Nippon Silica Glass Co., Ltd. for their contribution to this work in preparing the specimens, measuring the OH content, and providing the technical data.

[1] R. D. Maurer, Proc. IEEE **61**, 452 (1973).
[2] T. Li, IEEE J. Sel. Areas Commun. **SAC–1**, 356 (1983).
[3] H. Kanamori *et al.*, J. Lightwave Technol. **4**, 1140 (1986).
[4] M. Kawachi, Opt. Quantum Electron. **22**, 391 (1990).
[5] R. Brückner, J. Non-Cryst. Solids **5**, 123 (1970).
[6] T. Izawa, S. Sudo, and F. Hanawa, Trans. Inst. Electron. Commun. Eng. Jpn., Sect. E **62**, 779 (1979).
[7] G. Hetherington, K. H. Jack, and J. C. Kennedy, Phys. Chem. Glasses **5**, 130 (1964).
[8] Y. Kikuchi, H. Sudo, and N. Kuzuu, J. Ceram. Soc. Jpn. **105**, 645 (1997).
[9] S. Sakaguchi, S. Todoroki, and S. Shibata, J. Am. Ceram. Soc. **79**, 2821 (1996).
[10] N. Kuzuu and M. Murahara, Phys. Rev. B **47**, 3083 (1993).
[11] Technical data of Nippon Silica Glass Co., Ltd.
[12] N. P. Bansal and R. H. Doremus, *Handbook of Glass Properties* (Academic, New York, 1986), Chap. 10, pp. 306–336.
[13] W. P. Mason and H. J. McSkimin, J. Acoust. Soc. Am. **19**, 464 (1947).
[14] H. J. McSkimin, J. Appl. Phys. **24**, 988 (1953).
[15] S. Spinner, J. Am. Ceram. Soc. **39**, 113 (1956).
[16] S. Spinner, J. Am. Ceram. Soc. **45**, 394 (1962).
[17] O. L. Anderson and H. E. Bommel, J. Am. Ceram. Soc. **38**, 125 (1955).
[18] C. K. Jones, P. G. Klemens, and J. A. Rayne, Phys. Lett. **8**, 31 (1964).
[19] J. E. Shelby, Jr., and D. E. Day, J. Am. Ceram. Soc. **52**, 169 (1969).
[20] J. E. Shelby, Jr., and D. E. Day, J. Am. Ceram. Soc. **53**, 182 (1970).
[21] K. Nassau, J. W. Shiever, and J. T. Krause, J. Am. Ceram. Soc. **58**, 461 (1975).
[22] J. Kushibiki and N. Chubachi, IEEE Trans. Sonics Ultrason. **SU–32**, 189 (1985).
[23] J. Kushibiki, H. Asano, T. Ueda, and N. Chubachi, Proc. IEEE Ultrason. Symp., 1986, pp. 749–753.
[24] J. Kushibiki, T. Ueda, and N. Chubachi, Proc. IEEE Ultrason. Symp., 1987, pp. 817–821.

[25] M. Kadota, T. Kitamura, and T. Kasanami, Trans. IEE **111–C**, 412 (1991).
[26] C. K. Jen, C. Neron, A. Shang, K. Abe, L. Bonnell, and J. Kushibiki, J. Am. Ceram. Soc. **76**, 712 (1993).
[27] Y. Ono, J. Kushibiki, and N. Chubachi, Proc. IEEE Ultrason. Symp., 1993, pp. 1243–1246.
[28] J. Kushibiki and Y. Ono, IEEE Trans. Ultrason. Ferroelectr. Freq. Control (submitted).
[29] H. A. Bowman and R. M. Schoonover, J. Res. Natl. Bur. Stand., Sect. C **71**, 179 (1967).
[30] J. Kushibiki and M. Arakawa, IEEE Trans. Ultrason. Ferroelectr. Freq. Control **45**, 421 (1998).
[31] J. Kushibiki, N. Akashi, T. Sannomiya, N. Chubachi, and F. Dunn, IEEE Trans. Ultrason. Ferroelectr. Freq. Control **42**, 1028 (1995).
[32] J. Williams and J. Lamb, J. Acoust. Soc. Am. **30**, 308 (1958).
[33] J. Kushibiki and M. Arakawa, J. Acoust. Soc. Am. (submitted).
[34] I. A. Viktorov, *Rayleigh and Lamb Waves: Physical Theory and Applications* (Plenum, New York, 1967), Chap. I, pp. 46–57.
[35] J. J. Campbell and W. R. Jones, IEEE Trans. Sonics Ultrason. **SU–17**, 71 (1970).
[36] P. C. Schultz, Proc. IEEE **68**, 1187 (1980).
[37] Y. Ono, J. Kushibiki, and N. Chubachi (unpublished).